HOKKAIDO UNIVERSITY

Title	Parity reversal of 12 Be
Author(s)	Homma, H.; Isaka, M.; Kimura, M.
Citation	Physical Review C, 91(1), 14314 https://doi.org/10.1103/PhysRevC.91.014314
Issue Date	2015-01-16
Doc URL	http://hdl.handle.net/2115/58431
Rights	©2015 American Physical Society
Type	article
File Information	PhysRevC_91_014314.pdf

Instructions for use

Parity reversal of $^{12}_{\Lambda}$Be

H. Homma,[1] M. Isaka,[2] and M. Kimura[1]

[1]*Department of Physics, Hokkaido University, Sapporo 060-0810, Japan*
[2]*RIKEN Nishina Center, RIKEN, Wako, Saitama 351-0198, Japan*
(Received 14 October 2014; revised manuscript received 9 December 2014; published 16 January 2015)

We study the spectrum of $^{12}_{\Lambda}$Be by using an extended version of antisymmetrized molecular dynamics for hypernuclei. Our result indicates that the Λ-particle impurity effect causes the positive-parity ground state of $^{12}_{\Lambda}$Be to revert to the normal state, i.e., negative parity. This parity reversion is attributed to the difference in the Λ binding energy between the positive- and negative-parity states, which in turn originates in the difference in α clustering and deformation.

I. INTRODUCTION

Despite their short lifetime, hypernuclei have been a subject of particular interest in nuclear physics because they provide an almost unique opportunity to investigate underlying baryon-baryon interactions. In particular, knowledge of the interaction between a Λ hyperon and nucleons has greatly increased in recent decades [1–7], which strongly promotes the physics of hypernuclear many-body problems. A particularly interesting problem in hypernuclear many-body physics concerns the dynamical features of Λ hypernuclei manifested by adding a Λ particle to, for example, stabilize the system [8,9], modify the sizes [10–12], or deform and cluster [13–20]. Thus, hypernuclear many-body physics can be regarded as impurity physics because it offers a means to investigate nuclear dynamical responses to the addition of hyperons or nuclear structure by using hyperons as probes. We can expect forthcoming experiments to expand the domain of hypernuclear physics toward neutron-rich or heavier systems and thereby uncover many exotic phenomena caused by the Λ-impurity effect.

One such system of interest to be experimentally accessible is single-Λ hypernuclei of neutron-rich Be isotopes. More specifically, $^{12}_{\Lambda}$Be, which is accessible via the ^{12}C(π^-,K^+) reaction, is particular interesting because the core nucleus ^{11}Be is known to have a quite exotic structure. It has two bound states—one with positive parity and the other with negative parity. The ground state has positive parity, and the negative-parity state is 320 keV above the ground state [21–23]. Because the order of these two states contradicts the ordinary nuclear-shell ordering and the neutron-shell gap $N = 8$ is collapsed, this peculiar order of states is referred to as "parity inversion" or "breakdown of the $N = 8$ magic number." The question we address herein is how the Λ-impurity effect will modify the "parity reversion" in $^{12}_{\Lambda}$Be.

In this article, we predict that adding a Λ particle will cause the parity inversion in ^{11}Be to revert to "normal" (i.e., negative) parity in $^{12}_{\Lambda}$Be. This study is based on the theoretical framework of antisymmetrized molecular dynamics (AMD). AMD has been applied to investigate exotic phenomena in neutron-rich nuclei and has successfully described them such as the breakdown of the $N = 8$ and $N = 20$ magic numbers [24–29]. In the present study, we use an extended

version of AMD for hypernuclei (HyperAMD) to investigate $^{12}_{\Lambda}$Be. HyperAMD has already been applied to p-sd-shell hypernuclei [19,20], and its detailed formulation is given there.

II. FORMALISM

The Hamiltonian used in this study is

$$H = H_N + H_{\Lambda} - T_g, \tag{1}$$

$$H_N = T_N + V_{NN} + V_C, \quad H_{\Lambda} = T_{\Lambda} + V_{\Lambda N}, \tag{2}$$

where T_N, T_{Λ}, and T_g are the kinetic energies of the nucleons, Λ particle, and center-of-mass motion, respectively. We use the Gogny D1S interaction [30] as effective nucleon-nucleon interaction V_{NN}, and the Coulomb interaction V_C is approximated by the sum of seven Gaussians. To see the interaction dependence of the result, we tested various ΛN interactions for the central part of $V_{\Lambda N}$ [31–33], and in this paper we present the results obtained by the YN G-matrix interactions derived from the Nijmegen potentials named model D [7,34], NSC97f [35], and ESC08c [36], which we denote ND, NSC97f and ESC08c, respectively. Their strengths depend on the nuclear Fermi momentum k_F, and we adopt the value of $k_F = 1.06$ fm^{-1}, which is obtained by applying averaged density approximation [37]. As the spin-orbit interaction part of $V_{\Lambda N}$, we always used that of the ESC08c.

The variational HyperAMD wave function is a parity eigenstate. The intrinsic wave function Ψ_{int} is represented by the direct product of the Λ single-particle wave function φ_{Λ} and the wave function Ψ_N of A nucleons, which is a Slater determinant of the nucleon wave packets ψ_i,

$$\Psi^{\pm} = P^{\pm}\Psi_{\text{int}}, \quad \Psi_{\text{int}} = \Psi_N \otimes \varphi_Y, \tag{3}$$

$$\Psi_N = \frac{1}{\sqrt{A!}} \det\{\psi_i(\boldsymbol{r}_j)\}, \tag{4}$$

where $P^{\pm}$ is the parity projector. The nucleon single-particle wave packets ϕ_i are represented by a Gaussian:

$$\psi_i(\boldsymbol{r}) = \phi_i(\boldsymbol{r})\chi_i\tau_i, \tag{5}$$

$$\phi_i(\boldsymbol{r}) = \prod_{\sigma=x,y,z} \left(\frac{2\nu_{\sigma}}{\pi}\right)^{1/4} \exp\left\{-\nu_{\sigma}(r - Z_i)^2_{\sigma}\right\}, \tag{6}$$

$$\chi_i = a_i\chi_{\uparrow} + b_i\chi_{\downarrow}, \quad \tau_i = \text{p} \quad \text{or} \quad \text{n}. \tag{7}$$

The Λ single-particle wave function is represented by a sum of Gaussians,

$$\varphi_\Lambda(\mathbf{r}) = \sum_{m=1}^{M} c_m \varphi_m(\mathbf{r}), \quad \varphi_m(\mathbf{r}) = \phi_m(\mathbf{r})\chi_m, \quad (8)$$

$$\phi_m(\mathbf{r}) = \prod_{\sigma=x,y,z} \left(\frac{2\nu_\sigma}{\pi}\right)^{1/4} \exp\left\{-\nu_\sigma(r-\zeta_m)_\sigma^2\right\}, \quad (9)$$

$$\chi_m = \alpha_m \chi_\uparrow + \beta_m \chi_\downarrow, \quad (10)$$

where the number of superposed Gaussians is chosen to be sufficiently large to achieve energy convergence. The variational parameters are centroids of the Gaussian wave packets $\mathbf{Z}_i$ and ζ_m, the Gaussian width ν_σ, the coefficients c_m, and spin directions a_i, b_i, α_m, and β_m. These parameters are set to minimize the total energy under the constraint on the matter quadrupole deformation parameter β [24]. The value of β is constrained to range from 0 to 1.2 in intervals of 0.025.

After the variation, we project out the eigenstate of the total angular momentum J for each value of β,

$$\Psi_{MK}^{J\pm}(\beta) = \frac{2J+1}{8\pi^2} \int d\Omega D_{MK}^{J*}(\Omega) R(\Omega) \Psi^\pm(\beta). \quad (11)$$

The integrals over the three Euler angles Ω are performed numerically. Then we perform the generator coordinate method (GCM) [38]. The wave functions with differing values of K and β are superposed:

$$\Psi_n^{J\pm} = \sum_p \sum_{K=-J}^{J} c_{npK} \Psi_{MK}^{J\pm}(\beta_p). \quad (12)$$

The coefficients c_{npK} are determined by solving the Griffin-Hill-Wheeler equation.

III. RESULTS AND DISCUSSIONS

Before discussing $_\Lambda^{12}$Be, it is helpful to review the structure of ^{11}Be. Figure 1(a) shows the observed spectra of the $N = 7$ isotones, ^{13}C and ^{11}Be. The large gap between the $p_{1/2}$

FIG. 2. (Color online) Matter (ρ_m) and proton (ρ_p) density distributions for the bandhead states of ^{11}Be and $_\Lambda^{12}$Be. Color plots show the density distribution of the Λ particle.

and sd shells in ^{13}C collapses in ^{11}Be. The ^{11}Be ground state has positive parity, and the order of the $p_{1/2}$ and sd shells looks inverted, which is called *parity inversion* [21,22]. Using the original Gogny D1S parameter set, our calculation reproduces the spin-parity of the ground state and gives a binding energy of 65.32 MeV; the first excited state $1/2_1^-$ is at 540 keV (the observed values are 65.48 MeV and 320 keV, respectively [23]). For more quantitative discussion of $_\Lambda^{12}$Be, we weakened the spin-orbit interaction of Gogny D1S by 5% to exactly reproduce the observed $1/2_1^-$ excitation energy. With this modification, we calculate the binding energy of ^{11}Be to be 64.77 MeV, and the resulting spectrum is shown in Fig. 1(b). Here the excited unbound states are calculated within the bound-state approximation.

The low-lying states of Be isotopes are known to have a 2α cluster core and valence neutrons occupying the molecular orbits around the core, which are called π and σ orbits [26]. The formation of the 2α cluster core in each state is confirmed by the proton density shown in Fig. 2. The ground state is a member of the $K^\pi = 1/2^+$ band in which two of the three valence neutrons occupy the π orbit, and the third valence

FIG. 1. (Color online) (a) Observed spectra of ^{13}C and ^{11}Be. (b) Spectrum of ^{11}Be calculated by AMD. (c) Spectra of $_\Lambda^{12}$Be calculated by HyperAMD with the four different ΛN interactions given in the figure.

TABLE I. Calculated binding (B) and excitation E_x energies (MeV), matter quadrupole deformation β, and root-mean-square radii $r_{\rm rms}$ (fm) of the bandhead states of ^{11}Be and ^{12}Be. The results of $^{12}_{\Lambda}$Be are obtained by using ESC08c. The kinetic (T_Λ) and potential ($V_{\Lambda N}$) energies of Λ particle are also shown for $^{12}_{\Lambda}$Be. Numbers in parentheses are the observed data [39].

	J^π	B	E_x	β	$r_{\rm rms}$	B_Λ	T_Λ	$V_{\Lambda N}$
^{11}Be	$1/2_1^-$	64.45	0.32	0.52	2.53			
		(65.16)	(0.32)					
	$1/2_1^+$	64.77	0	0.72	2.69			
		(65.48)	(0)		(2.73)			
	$3/2_1^-$	62.72	2.05	0.90	2.98			
$^{12}_{\Lambda}$Be	0_1^-	75.29	0.00	0.47	2.51	10.84	7.01	-17.87
	0_1^+	75.11	0.18	0.70	2.67	10.34	6.98	-17.43
	1_3^-	71.62	3.67	0.87	2.94	8.90	6.58	-15.62

neutron occupies the σ orbit. In terms of the spherical shell model, a neutron is promoted to sd shell across the $N = 8$ shell gap (breakdown of magic number $N = 8$). The first excited state has negative parity and belongs to the $K^\pi = 1/2^-$ band. All valence neutrons occupy the π orbit or p shell, which corresponds to the normal shell order. As we can see from Fig. 2 and Table I, the ground state has a more pronounced 2α clustering and a larger quadrupole deformation β than the first excited state. Here the quadrupole deformation β of each state is defined as the deformation of the basis wave function $\Psi_{MK}^{J\pm}(\beta)$ that has maximum overlap with the GCM wave function [Eq. (12)]. Among the bandhead states, the $3/2_1^-$ state (bandhead of $K^\pi = 3/2^-$) with two valence neutrons in a σ orbit is the most deformed. The assignment of the unbound excited states, including the $3/2_1^-$ state, is still under discussion, so we devolve further discussions to Refs. [40–42]. Here we simply note that the positive-parity ground state is more deformed than the first excited state with negative parity. This point makes a difference when a Λ particle is injected.

We found that all of the ΛN interactions tested in the present study yield the same qualitative result for $^{12}_{\Lambda}$Be and predict the negative-parity ground state of $^{12}_{\Lambda}$Be. In other words, the inverted ground-state parity of ^{11}Be will be reverted in $^{12}_{\Lambda}$Be by injecting a Λ particle. The spectra of $^{12}_{\Lambda}$Be obtained by using ESC08c, ND, and NSC97f are shown in Fig. 1(c). Among the tested ΛN interactions, the ND gives the largest energy gap between the negative-parity ground state and the positive-parity excited state, while the NSC97f gives the smallest. For the moment, we focus on the result obtained by using the ESC08c, and later we discuss the quantitative difference and ΛN interaction dependence of the results.

All states shown in Fig. 1(c) have a Λ in an s orbit and are classified into three bands. They are generated by the coupling of the $K^\pi = 1/2^+, 1/2^-$, and $3/2^-$ bands of ^{11}Be with a Λ particle in an s orbit; thus, there are always doublet states of $^{12}_{\Lambda}$Be for each corresponding state of ^{11}Be. These bands are denoted as $K^\pi = 1/2^+ \otimes \Lambda_s, 1/2^- \otimes \Lambda_s$, and $3/2^- \otimes \Lambda_s$, respectively. In the case of the ESC08c, the ground doublet has a ^{11}Be$(1/2_1^-) \otimes \Lambda_s$ configuration and consists of the 0_1^- and 1_1^- states with binding energies of 75.29 and 75.27 MeV, while
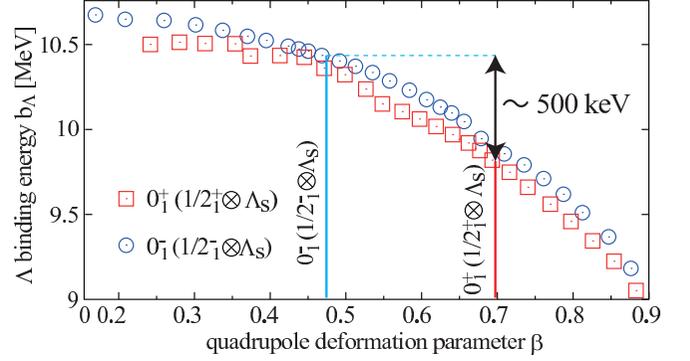

FIG. 3. (Color online) The Λ binding energy of the 0_1^- and 0_1^+ states as function of proton quadrupole deformation parameter β. Lines in the figure denote the deformation parameter of $0_1^\pm$ states given in Table I.

the first excited doublet with a ^{11}Be$(1/2_1^+) \otimes \Lambda_s$ configuration consists of the 0_1^+ state at 180 keV and the 1_1^+ state at 220 keV. Thus, the ground-state parity has reverted to negative parity in $^{12}_{\Lambda}$Be, as if adding a Λ particle has restored the $N = 8$ shell gap. This parity reversion of $^{12}_{\Lambda}$Be is due to the difference in the Λ particle binding energy B_Λ for the ground and first excited doublets. Here B_Λ is defined as the difference in binding energies between a given $^{12}_{\Lambda}$Be and the corresponding ^{11}Be state,

$$B_\Lambda = B(^{12}_{\Lambda}{\rm Be}(J^\pi)) - B(^{11}{\rm Be}(J'^\pi)), \qquad (13)$$

and as shown in Table I, B_Λ of the 0_1^- state is 500 keV larger than that of the 0_1^+ state. The change of the core nucleus energy H_N caused by injection of a Λ particle is rather small; therefore, the difference in B_Λ overwhelms the energy difference between the $1/2_1^\pm$ states of ^{11}Be, leading to the parity reversion in $^{12}_{\Lambda}$Be. This difference in B_Λ mainly arises from the ΛN potential $V_{\Lambda N}$ as shown in Table I. In turn, the difference in the ΛN potential $V_{\Lambda N}$ originates in the difference in quadrupole deformation. Figure 3 shows the Λ particle binding energies for the $0_1^\pm$ states as a function of quadrupole deformation, which is defined as the expectation value of H_Λ by the angular-momentum-projected wave functions for each deformation parameter β,

$$b_\Lambda^\pm(\beta) = -\langle \Psi^{0\pm}(\beta)|H_\Lambda|\Psi^{0\pm}(\beta)\rangle. \qquad (14)$$

The b_Λ of the 0_1^+ and 0_1^- states rapidly decrease as the deformation becomes larger, which is mostly due to the reduction of $V_{\Lambda N}$ caused by the decrease of the overlap between the Λ particle and the nucleons wave functions, as discussed in the case of p-sd-pf shell nuclei [19,20,43]. The results shown in Fig. 3 allow us to confirm that the 500-keV difference in B_Λ originates from the different deformation of the $0_1^\pm$ states. Because the $3/2_1^-$ state is the most deformed among the bandhead states of ^{11}Be, the 1_3^- state (^{11}Be$(3/2_1^-) \otimes \Lambda_s$) has the smallest B_Λ and its excitation energy is considerably shifted up.

Adding a Λ particle slightly modifies the structure of the ^{11}Be core nucleus. The attraction of the Λ particle sitting at the center of the system causes the intercluster distance between

the 2α clusters to decrease (Fig. 2), and it also leads to the a decrease in the deformation and radius (Table I). In spite of the neutron-halo structure of ^{11}Be, this reduction is rather small compared with what is observed for $^{7}_{\Lambda}$Li [12] and cannot be clearly seen in the density distribution (Fig. 2). We attribute this to the presence of valence neutrons occupying molecular orbits in $^{12}_{\Lambda}$Be. A decrease in the distance between the 2α clusters would result in the valence neutrons in π or σ orbits loosing their binding energy [26]. Consequently, the valence neutrons effectively serve to prevent a drastic reduction of the 2α distance. Note that this also explains why the change in the expectation value of the nuclear part is not large compared to the difference in B_{Λ}.

Finally, we examine how the properties and uncertainties of the ΛN interactions affect the quantitative results and the parity reversion in $^{12}_{\Lambda}$Be. The first point we focus on is the spin-independent odd-parity part of the ΛN central force that acts between the Λ particle in s orbit and nucleons in p orbits. Recall that the $1/2^{-}_{1}$ state of ^{11}Be has 7 nucleons in the p orbits, whereas the $1/2^{+}_{1}$ state has 6 nucleons. Therefore, roughly speaking, the 0^{-}_{1}-1^{-}_{1} doublet has greater number of spin-independent odd-parity interactions between the Λ particle and nucleons (7 interactions) than the 0^{+}_{1}-1^{+}_{1} doublet (6 interactions). Consequently, we can imagine if the spin-independent odd-parity interaction is too strongly repulsive, the centroid energy of the 0^{-}_{1}-1^{-}_{1} doublet will be pushed up relative to the 0^{+}_{1}-1^{+}_{1} doublet and the parity reversion will not occur. It is known that this interaction is more repulsive in NSC97f than in ESC08c, while it is attractive in ND. This difference can be seen in Fig. 1 (c), i.e., NSC97f gives smaller centroid energy difference (0.14 MeV) than ESC08c (0.19 MeV), while ND gives the largest difference (0.34 MeV).

The second point is the $\boldsymbol{\sigma}_{\Lambda} \cdot \boldsymbol{\sigma}_{N}$ dependent part of the central force and the spin-orbit force, which apparently affects the energy splitting within a doublet. It is also known that NSC97f has stronger $\boldsymbol{\sigma}_{\Lambda} \cdot \boldsymbol{\sigma}_{N}$-dependent term than ESC08c and ND and reproduces the observed doublet splitting in $^{4}_{\Lambda}$H and $^{7}_{\Lambda}$Li [44]. This characteristic is also confirmed in Fig. 1, in which NSC97f gives the largest doublet splitting. As a result of the spin-independent odd-parity and $\boldsymbol{\sigma}_{\Lambda} \cdot \boldsymbol{\sigma}_{N}$-dependent parts, the energy gap between the 1^{-}_{1} and 0^{+}_{1} is only 40 keV in

NSC97f result. It is noted that the sign of the positive- and odd-parity $\boldsymbol{\sigma}_{\Lambda} \cdot \boldsymbol{\sigma}_{N}$-dependent part of ND is opposite to those of NSC97f and ESC08c. In Fig. 1(c), this difference leads to the opposite level ordering of the the 0^{-}_{1}-1^{-}_{1} and 0^{+}_{1}-1^{+}_{1} doublets between the ND and NSC97f results, while these doublets are almost degenerated in the ESC08c result. It is found that the contribution from the spin-orbit interaction of ESC08c is less than 100 keV for $0^{\pm}_{1}$ and $1^{\pm}_{1}$ doublets, which is consistent with the observations in $^{9}_{\Lambda}$Be [45,46] and $^{13}_{\Lambda}$C [47,48]. Therefore, we consider that the uncertainty of the spin-orbit interaction has minor influence to the parity reversion compared to other uncertainties discussed above. Although all the ΛN interactions tested in this study suggest that the reversion will occur, several properties of the ΛN interactions have influence to the parity reversion in $^{12}_{\Lambda}$Be, and more detailed knowledge on ΛN interaction such as tensor term will be needed for further quantitative studies.

IV. CONCLUSION

In summary, we have investigated the low-lying states of $^{12}_{\Lambda}$Be by using the HyperAMD. We predict a parity reversion of $^{12}_{\Lambda}$Be; that is the inverted ground-state parity of ^{11}Be reverts to "normal" (i.e., negative) parity in $^{12}_{\Lambda}$Be. The parity reversion is caused by the different deformations of the ground and first excited states of ^{11}Be, which lead to a difference in the Λ particle binding energy B_{Λ}. In addition, the parity reversion suggests that it may be possible to probe the different deformations of the ground and first excited states of ^{11}Be by adding a Λ-particle impurity. Therefore, it is quite interesting and important to investigate the excitation spectrum of $^{12}_{\Lambda}$Be by the $^{12}C(\pi^{-}, K^{+})$ reaction with high-energy resolution.

[1] M. N. Nagels, T. A. Rijken, and J. J. de Swart, Phys. Rev. D **12**, 744 (1975).

[2] Y. Yamamoto and H. Bandō, Prog. Theor. Phys. **69**, 1312 (1983).

[3] D. J. Millener, A. Gal, C. Dover, and R. Dalitz, Phys. Rev. C **31**, 499 (1985).

[4] A. Reuver, K. Holinde, and J. Speth, Nucl. Phys. A **570**, 543 (1994).

[5] T. A. Rijken and Y. Yamamoto, Phys. Rev. C **73**, 044008 (2006).

[6] Y. Fujiwara, Y. Suzuki, and C. Nakamoto, Prog. Part. Nucl. Phys. **58**, 439 (2007).

[7] M. M. Nagels, T. A. Rijken, and J. J.d e Swart, Phys. Rev. D **15**, 2547 (1977); **20**, 1633 (1979).

[8] A. Mondragón and E. Hernández, Phys. Rev. C **41**, 1975 (1990).

[9] H. Ohkura, T. Yamada, and K. Ikeda, Prog. Theor. Phys. **94**, 47 (1995).

[10] T. Motoba, H. Bando, and K. Ikeda, Prog. Theor. Phys. **70**, 189 (1983).

[11] E. Hiyama, M. Kamimura, K. Miyazaki, and T. Motoba, Phys. Rev. C **59**, 2351 (1999).

[12] K. Tanida *et al.*, Phys. Rev. Lett. **86**, 1982 (2001).

[13] T. Yamada, K. Ikeda, H. Bandō, and T. Motoba, Prog. Theor. Phys. **71**, 985 (1984).

[14] T. Sakuda and H. Bandō, Prog. Theor. Phys. **78**, 1317 (1987).

[15] M. T. Win and K. Hagino, Phys. Rev. C **78**, 054311 (2008).

[16] H.-J. Schulze, M. T. Win, K. Hagino, and H. Sagawa, Prog. Theor. Phys. **123**, 569 (2010).

[17] E. Hiyama, M. Kamimura, T. Motoba, T. Yamada, and Y. Yamamoto, Phys. Rev. Lett. **85**, 270 (2000).

[18] E. Hiyama, M. Kamimura, Y. Yamamoto, and T. Motoba, Phys. Rev. Lett. **104**, 212502 (2010).

[19] M. Isaka, M. Kimura, A. Dóte, and A. Ohnishi, Phys. Rev. C **83**, 044323 (2011).

[20] M. Isaka, M. Kimura, A. Dóte, and A. Ohnishi, Phys. Rev. C **83**, 054304 (2011).

[21] D. H. Wilkinson and D. E. Alburger, Phys. Rev. **113**, 563 (1959).

[22] I. Talmi and I. Unna, Phys. Rev. Lett. **4**, 469 (1960).

[23] F. Ajzenberg-Selove, Nucl. Phys. A **248**, 1 (1975).

[24] A. Dote, H. Horiuchi, and Y. Kanada-En'yo, Phys. Rev. C **56**, 1844 (1997).

[25] Y. Kanada-En'yo and H. Horiuchi, Phys. Rev. C **66**, 024305 (2002).

[26] W. von Oertzen, M. Freer, and Y. Kanada-En'yo, Phys. Rep. **432**, 43 (2006), and references therein.

[27] Y. Kanada-En'yo, M. Kimura, and H. Horiuchi, C. R. Phys. **4**, 497 (2003).

[28] M. Kimura and H. Horiuchi, Prog. Theor. Phys. **111**, 841 (2004).

[29] M. Kimura, Phys. Rev. C **75**, 041302 (2007).

[30] J. Dechargé and D. Gogny, Phys. Rev. C **21**, 1568 (1980).

[31] Y. Yamamoto, T. Motoba, H. Himeno, K. Ikeda, and S. Nagata, Prog. Theor. Phys. **117**, 361 (1994).

[32] E. Hiyama, M. Kamimura, T. Motoba, T. Yamada, and Y. Yamamoto, Prog. Theor. Phys. **97**, 881 (1997).

[33] E. Hiyama, M. Kamimura, Y. Yamamoto, T. Motoba, and T. A. Rijken, Prog. Theor. Phys. Suppl. **185**, 106 (2010).

[34] T.A. Rijken, P. M. M. Maessen, and J. J. de Swart, Nucl. Phys. A **547**, 245 (1992).

[35] T. A. Rijken, V. G. J. Stoks, and Y. Yamamoto, Phys. Rev. C **59**, 21 (1999).

[36] T. Rijken, M. Nagels, and Y. Yamamoto, Prog. Theor. Phys. Suppl. **185**, 14 (2010); Genshikaku Kenkyu **57**(Suppl. 3), 6 (2013).

[37] Y. Yamamoto, T. Motoba, and T. A. Rijken, Prog. Theor. Phys. Suppl. **185**, 72 (2010).

[38] D. L. Hill and J. A. Wheeler, Phys. Rev. **89**, 1102 (1953); J. J. Griffin and J. J. Wheeler, *ibid.* **108**, 311 (1957).

[39] A. Ozawa, T. Suzuki, and I. Tanihata, Nucl. Phys. A **693**, 32 (2001).

[40] M. Freer *et al.*, Nucl. Phys. A **834**, 621c (2010).

[41] W. A. Peters *et al.*, Phys. Rev. C **83**, 057304 (2011).

[42] H. T. Fortune and R. Sherr, Phys. Rev. C **83**, 054314 (2011).

[43] M. Isaka, K. Fukukawa, M. Kimura, E. Hiyama, H. Sagawa, and Y. Yamamoto, Phys. Rev. C **89**, 024310 (2014).

[44] E. Hiyama, Y. Yamamoto, Th. A. Rijken, and T. Motoba, Phys. Rev. C **74**, 054312 (2006).

[45] M. May *et al.*, Phys. Rev. Lett. **51**, 2085 (1983).

[46] H. Akikawa *et al.*, Phys. Rev. Lett. **88**, 082501 (2002).

[47] S. Ajimura *et al.*, Phys. Rev. Lett. **86**, 4255 (2001).

[48] H. Kohri *et al.*, Phys. Rev. C **65**, 034607 (2002).